Chapter Three *Fundamentals of VCSELs*

Vertical-Cavity Surface-Emitting Lasers (VCSELs) is going to be future semiconductor laser device for communication applications. This is significant achievements because at the beginning of the 1990s this device was considered as part of laboratory novelties. The development is due to the major improvements on device performance and the compatibility with low-cost wafer scale fabrication and characterization techniques. In this chapter, the VCSELs developments, device advantages, basic operation, materials and fabrication, device structure and design are briefly reviewed, with their applications introduced.

3.1 VCSELs Development

The development of VCSELs is summarized in Table 3.1. The VCSELs idea was invented in 1977 with the first device came out in 1979 [22] based on InGaAsP-InP at 1.3 μm. Device improvements were made by 1986 [39] using GaAs. The first room-temperature CW GaAs-based device was demonstrated in 1988 [40]. In 1989, a GaInAs VCSELs exhibiting a 1-2 mA threshold current was demonstrated [41]. Since 1992, GaAs-based VCSELs have been extensively studied with 780, 850 and 980 nm devices are now commercialized into optical applications. Introduction of wafer-fusion technique [42] allowed operation of 1.55 μm VCSELs at higher temperature. In 1993, room temperature CW red AlGaInAs device was developed [43] followed by green-blue-ultraviolet VCSELs research starting 1996 [44, 45].

Table 3.1: History of VCSELs research.

I	1977-1987	Early ideas & Initial demonstrations
II	1988-1998	CW & Device study
III	1999 till present	Production & Extension of applications

3.2 Advantages of VCSELs over EELs

VCSELs offer various advantages in comparison to EELs as discussed below. These advantages make VCSELs promising device for many optoelectronics applications. Appendix A gives a technical comparison of VCSELs, EELs and LED.

3.2.1 *Fiber coupling efficiency*

Due to the device geometry as described in Chapter Two, VCSELs emits circular output beam that is readily coupled into fiber core which is generally circular in cross section as shown in Figure 3.1. It is capable of achieving coupling efficiency of 80% without additional lenses that EELs required to achieve acceptable efficiency.

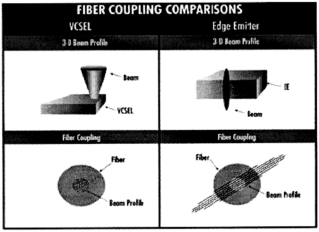

Figure 3.1: Fiber coupling comparisons between VCSELs and EELs.

3.2.2 *Emission capability*

The device geometry of VCSELs results in surface emission which is perpendicular to the wafer plane. This surface emission capability allow VCSELs to be designed anywhere linearly on the wafer chip, making 2D arrays applications possible.

PERPUSTAKAAN UNIVERSITI MALAYA

3.2.3 *Operating mode*

VCSELs have a short cavity length; hence the longitudinal mode spacing is large. Plus, there is only one longitudinal mode in the gain linewidth producing single longitudinal mode operation. In EELs, due to the large cavity length, the longitudinal mode spacing is small compared to the linewidth of the gain. This results lasing operation on multiple longitudinal modes. Mode-hopping can occurs due to temperature or current changes where data can jump from one mode to other besides reducing light intensity of each longitudinal mode due to mode competition.

3.2.4 *Low threshold current operation*

VCSELs used a very thin active region, applying only a small volume of active material. Thus, only a small injected current is needed, allowing lower threshold current. VCSELs typically needs low threshold current (below 10 mA) to operate.

3.2.5 *Manufacturing efficiency*

VCSELs can be tested in wafer form before dicing and packaging, where the reliability and functionality are tested with minimal cost. On-wafer testing capability allows defective chips to be identified early, thus increasing manufacturing yields and reducing cost. EELs must be cleaved and packaged before any testing can be done, and this will increase the manufacturing cost. VCSELs wafer-scale processing methods are also similar to silicon integrated circuits industry.

3.2.6 *Component integration*

The small size and planar structure of VCSELs offers integration with other components such as driver circuits, photodetectors and heat sinks on the same wafer, or integration by using flip-chip bonding or other standard packaging methods.

3.2.7 *Stable operation*

VCSELs also have very stable performance characteristics over temperature. This allows the monitor photodiode feedback loop to be eliminated in many applications, thus simplifying the ICs and packaging design.

3.3 VCSELs Basic Operation

The fundamental operation of the VCSELs is identical to EELs that is both operate on the principle of an optical gain medium and reflective mirrors. EELs have higher gain per unit length because the light beam passes horizontally through the active region compared to VCSELs where the light beam travels vertically. Instead of using cleaving to create mirror facets as in EELs, VCSELs use alternating layers of epitaxial materials with alternating indices of refraction, as shown in Figure 3.2.

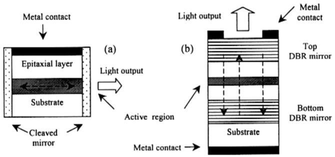

Figure 3.2: Basic operation difference between (a) EELs and (b) VCSELs. The dashed arrow inside the schematic devices shows the path of light beam propagation.

These layers form a DBR mirror with a reflectivity exceeds 99%. Because of the extremely low gain provided by the low gain per pass of VCSELs, the mirror must exhibit high reflectivity to compensate the optical loss. The top mirror is obviously designed with a lower reflectivity to allow the emission light to exit the cavity. Since the VCSELs mirrors are above and below the gain medium rather than to sides for EELs, light will exit the VCSELs from the top, rather than the edge as for EELs.

3.4 VCSELs Material and Fabrication

VCSELs materials are mainly based on group III-V element. If dielectric DBR mirror is employed, the material will be based on amorphous semiconductors. Table 3.2 summarized material extensively used or studied for each wavelength range with the development and difficulties.

Table 3.2: VCSELs material for various wavelength ranges.

Wavelength range	Visible blue (0.45-0.49 μm)	Visible green (0.49-0.58 μm)	Visible red (0.62-0.78 μm)	Infra-red (0.78-1.00 μm)	Long wavelength (1.30-1.55 μm)
Active material	InGaN	InGaN	InAlGaP	GaAs, InGaAs	InGaAsP
Mirror material	GaN/AlGaN	GaN/AlGaN	AlGaAs/AlAs	AlGaAs/AlAs	InGaAsP/InP, GaAs/AlAs, Dielectric
Substrate	Sapphire, SiC	Sapphire, SiC	GaAs	GaAs	InP, GaAs
Development stage	Research	Research	In near future production	Already in production	Initial research
Main difficulties	Epitaxy tech.	Epitaxy tech.	High temperature operation	No major problems	Mirror tech. & High temperature op.

The growth of VCSELs wafers is very demanding since the thickness, composition and uniformity control of numerous thin layers has to be accurate. Due to the epitaxial complexity, VCSELs development has depended on progress in compound semiconductor growth technology. In practice, VCSELs have been fabricated commonly by using three different epitaxy techniques that exhibit atomic precision control which are Molecular Beam Epitaxy (MBE), Gas-source Molecular Beam Epitaxy (GSMBE) and Metal-organic Chemical Vapor Deposition (MOCVD). The early development of VCSELs focused on MBE because of its superior precision control. By the end of 1980s, the high optical efficiency of the materials used in MOCVD had made it the choice for producing LED and laser diode. The rapid growth rate, high wafer throughput, run-to-run stability and wafer uniformity make MOCVD the preferable VCSELs manufacturing platform. Furthermore, the flexibility of materials and dopants that can be employed, and the ease of continuous composition grading, contributes to the growing usage of MOCVD.

3.5 VCSELs Structure

VCSELs are made by depositing multi-layers of semiconductor materials to form a cavity structure perpendicular to the substrate. Figure 3.3 shows structure of VCSELs device. Each of the structure will be described in the next section. In general, the pcontact and n-contact layers represent the metal contact region for electrical conduction, as well as defining the size of the cavity aperture. The substrate functions as platform growth and can act as heat sink. Mirror cavity is formed by the p- and n-DBR mirrors with the active region in between. Although not shown, this region composed of several QW. The active region is embedded between n- and p-spacers.

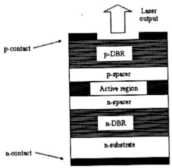

Figure 3.3: Schematic structure of VCSELs device.

3.5.1 *Distributed Bragg Reflector (DBR)*

DBR serves a dual role that is as highly reflective mirror and providing the pathway for current injection. The design of DBR is thus a trade-off between enabling high reflectivity for the mirror along with lowest possible resistance for both electrons and holes transported to the active region. Typical DBR consist of multi pairs of alternating low- and high-index quarter-wave thickness layers. The total number of periods in the DBR determines the reflectivity of the mirror. The bottom DBR (high reflector) is usually designed for a total reflectivity of >99.9%, while the top DBR (output coupler) is designed with reflectivity of 99.6%-99.9% [46]. Many different mirror systems have been proposed and demonstrated for the 1.55 μm VCSELs. It can be classified into three main categories which are epitaxially-grown, dielectric-deposited and wafer-fused. Figure 3.4 shows plot of reflectivity (at 1.55 μm) for the three different mirror systems versus the number of mirror periods, respectively.

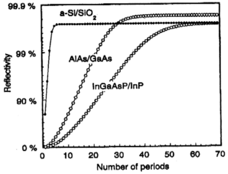

Figure 3.4: Comparison of reflectivity in 1.55 μm VCSELs DBR mirror systems.

3.5.1(a) *Epitaxially-grown mirror*

Epitaxially grown mirror based on compound III-V alloys exhibit a relatively small range of refractive index values ($2.9 \leq n \leq 3.5$) [47] and a moderate range of thermal conductivities ($0.02 \leq \kappa \leq 0.9$ W/cmK) [48]. Table 3.3 show selected material combinations that can be used for VCSELs for 1.55 μm wavelength.

Table 3.3: Epitaxial mirror tuned to 1.55 μm. Each mirror contains high-index and low-index material, thermal conductivity (W/cmK) and refractive index values. The row-column crossing corresponds to the fractional refractive index ($\Delta n / \bar{n}$) percentage. Refs: [46].

Low index	→		AlAs	$Al_{0.67}Ga_{0.33}As$	$AlAs_{0.56}Sb_{0.44}$	$AlP_{0.4}Sb_{0.6}$	$Al_{0.48}In_{0.52}As$	InP
High index	κ	→	0.91	0.16	0.057	0.039	0.045	0.68
↓	↓	n	2.89	3.04	3.10	3.05	3.21	3.17
GaAs	0.44	3.37	15.2%	10.3%	—	—	—	—
InGaAsP	0.045	3.45	—	—	10.7%	12.3%	7.2%	8.5%
AlInGaAs	0.045	3.47	—	—	11.3%	12.9%	7.8%	9%
AlGaAsSb	0.062	3.6	—	—	15%	16.5%	—	—
AlGaPSb	0.046	3.55	—	—	13.5%	15.2%	—	—

Epitaxially-grown mirrors have the obvious advantage that it can directly integrated with the InP- and GaAs-based VCSELs, allowing easy manufacturability and device fabrication. However, the main advantage of epitaxial mirror is that it can be made conductive by doping. The design of any epitaxial mirror that is also considered for current supply involves the optimization between the reflectivity and the electrical resistance. These two parameters are connected through the doping, which affects the absorption and the mirror conductivity. Several materials have been demonstrated for epitaxial mirror application such as InGaAsP/InP [49], GaAs/AlGaAs [50], AlGaAsSb/AlAsSb [51] and AlInGaAs/AlInAs [52].

3.5.1(b) <u>*Dielectric-deposited mirror*</u>

Dielectric-deposited mirror offers wide range of materials and refractive indexes where the amorphous semiconductor materials used can be deposited by various techniques such as electron-beam evaporation, sputtering and plasma-enhanced chemical-vapor deposition (PECVD). These materials are electrically insulating but exhibit a large range of thermal conductivities ($0.01 \leq \kappa \leq 2.5$ W/cmK) [46]. Table 3.4 displays selected amorphous material for VCSELs at 1.55 μm.

Table 3.4: Amorphous mirrors tuned to 1.55 μm. Each mirror contains high-index and low-index material, thermal conductivity and refractive index values. The row-column crossing corresponds to the fractional refractive index ($\Delta n/\bar{n}$) percentage. Refs: [53].

	Low index	→	MgF	CaF_2	SiO_2	MgO	Al_2O_3	Si_3N_4	TiO_2
High index	κ [W/cmK]	→	—	0.1	0.012	0.53	0.36	0.16	0.09
↓	↓	*n*	1.35	1.43	1.45	1.71	1.74	2.0	2.44
a-Si	0.026	3.6	91%	86%	85%	71%	70%	57%	38%
SiC	2.5	2.57	62%	57%	56%	40%	39%	25%	5%
ZnSe	0.19	2.46	58%	53%	52%	36%	34%	21%	1%
TiO_2	0.09	2.44	58%	52%	51%	35%	33%	20%	—
Si_3N_4	0.16	2.0	39%	33%	32%	16%	14%	—	—
Al_2O_3	0.36	1.74	25%	20%	18%	2%	—	—	—
MgO	0.53	1.71	24%	18%	16%	—	—	—	—

Due to high refractive index ratio, the dielectric-mirror usually only requires less than eight periods to achieve desirable reflectivity as shown in Figure 3.4. This high ratio produces small penetration depth thus reduces diffractive losses allowing for smaller devices to be fabricated. The most common material used is a-Si/SiO_2 where the typical absorption coefficient for a-Si is $\alpha \approx 100$ cm^{-1} at 1.55 μm [54]. In addition to the material absorption, the thermal conductivity for both of these materials are quite low, $\kappa \approx 0.012$ W/cmK for a-SiO_2 [55] and $\kappa \approx 0.026$ W/cmK for a-Si [56]. The thermal conductivity in amorphous semiconductor is generally poor, thus cannot be used as bottom, heat transferring mirror in VCSELs. The recent application of a-SiC/MgO [57] and a-

Si/Al_2O_3 [58] mirrors has dramatically improved VCSELs performance. Despite this, the refractive indexes of both MgO and Al_2O_3 are higher than SiO_2, and therefore the maximum reflectivity of mirror employing these two materials is lower than the a-Si/SiO_2, thus more periods are needed to achieve higher reflectivity. Another disadvantage of dielectric-mirror is that more complicated current injection schemes are required due to its electrically insulating characteristic.

3.5.1(c) *Wafer-fused mirror*

Fusion-bonding technology in VCSELs is similar to silicon-direct bonding [59], but with different bond properties [60], enabling the fabrication of devices by bonding of two semiconductors with different lattice constants. Fusion-bonding technology in VCSELs was realized by using single-fused interface to integrate a GaAs/AlAs mirror with InGaAsP active region at 1.3 μm VCSELs [61]. Further improvement on the single-fused device has been demonstrated at 1.55 μm by bonding GaAs/AlAs mirror to InGaAsP/InP mirror and active region [62]. Figure 3.5 shows the wafer-fusion process. The highest performance VCSELs to date has been employing double-fused structure [63] where InGaAsP active region is sandwiched between GaAs/AlGaAs mirrors.

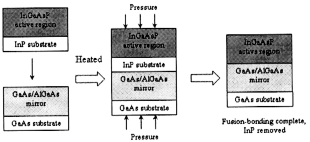

Figure 3.5: Schematic of wafer-fusion process.

This solved the lattice mismatched problem in integrating InGaAsP-based active region with GaAs/AlGaAs, which is the best material system for epitaxial-grown mirror. However, wafer-fusion mirror still contains many issues that need to be investigated.

The electrical, thermal and optical properties of this junction are highly dependent on the bonding process conditions and surface preparations. The cost of wafer consumption in wafer-fusion can also have effect on the manufacturing level.

3.5.2 *Active region*

The DBR mirrors and optical cavity are doped such that the active region is located at the p-n junction of the laser diode. Figure 3.6 illustrated the active region consists of multiple QW. The active region is placed within the optical cavity and overlaps the antinodes of the electromagnetic fields, providing optimal optical gain for the VCSELs.

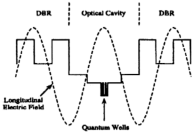

Figure 3.6: The refractive index profile and the longitudinal electric field in the optical cavity within VCSELs.

The requirement for long-wavelength VCSELs active region is more demanding than EELs. VCSELs devices typically have shorter gain region and high thermal resistance than EELs, which becomes more critical at operating temperature of 70^0-85^0C for fiber-optics operation. In addition, the performance of semiconductor laser is affected by Auger recombination, carrier leakage and carrier-related optical losses at longer wavelength [64, 65]. However, developments of active region materials and designs for 1.3 and 1.55 μm VCSELs operating above room temperature have been demonstrated recently as discussed below. Novel concepts such as quantum-dot active region is reported for VCSELs [66] where it offers improvement on carrier confinement and the potential for scaling smaller devices. Basically, VCSELs active region can be classified into InP- and GaAs-grown.

3.5.2(a) *InP-based active region*

The InGaAsP material is commonly used for emission in the long-wavelength range. InP-based EELs have been studied and applied extensively in fiber-optics networks, where the knowledge has carried over into VCSELs. Early long-wavelength VCSELs active regions consisted of bulk InGaAsP, with QW introduced later [67]. The high differential gain and low carrier density of QW active region [65] have provided method to realize CW operation at elevated temperatures. It is desirable to use a large number of QW due to high gain requirements of VCSELs. The highest reported operating temperature of 85^0C for long-wavelength VCSELs was achieved using strain compensated QW InGaAsP active region [68]. However, the InP system suffers from low characteristic temperatures compared to GaAs-based lasers. At 1.3-1.55 μm, laser performance is reduced by high Auger recombination, intervalence band absorption, poor thermal conductivity, carrier leakage and free carrier absorption [64, 65]. Nevertheless, much groundwork has been laid for VCSELs active region designs through progress in InP-based EELs employing strained QW. An alternative to InGaAsP is AlInGaAs lattice-matched to InP. The conduction band offset for AlInGaAs is higher than InGaAsP [69, 70] resulted in a deeper QW which produced high temperature operation and higher gain coefficient in EELs. As for long wavelength VCSELs, AlInGaAs active region demonstrated CW operation at temperature up to 40^0C [71] with submiliampere thresholds [72]. Multiple AlInGaAs active region also exhibited high differential efficiency [73], thus reducing the DBR requirement of obtaining high reflectivity. The lifetime of devices with Al-containing active region may become the drawback, although long lifetime device has been recently reported for EELs [74].

3.5.2(b) *GaAs-based active region*

The epitaxial and fabrication maturity of short-wavelength GaAs-based VCSELs have inspired GaAs application for long-wavelength active region where CW operation of 1.3 μm VCSELs with a GaInNAs active region was reported [75]. However, there is a problem in epitaxial growth where incorporation of N into the quaternary material is difficult especially in longer-wavelength device. In addition, threshold current density is high for emission wavelength above 1.2 μm. Progress in countering these problems are on development [76]. Alternatively, GaAsSb active regions have also been studied for long-wavelength VCSELs [77] with room temperature CW operation at 1.23 μm reported [78].

3.5.3 *Spacer*

In VCSELs structure, spacers are embedded between the active region and both the n- and p- DBR mirrors, respectively. The spacers reveal improvements in thermal resistance, transverse single mode behaviour and also for obtaining low resistance even for low doping levels which minimize absorption. These spacer regions help lower the resistance of the DBR by reducing the barriers to current flow in the conduction and valence bands. In addition, thermal resistance decreases continually with increasing spacer length because the additional structure of the spacer acts as a heat-spreading layer, which reduces the amount of heat accumulated in the active region area.

PERPUSTAKAAN UNIVERSITI MALAYA

3.6 VCSELs Device Design

In addition to the choices of materials for both mirrors and active region, there are numerous other design issues for optimizing VCSELs performance such as the current or mode confinement scheme and the ability for small scaling device. Figure 3.8 shows

A511931850

various current confinement schemes for VCSELs. Proton implantation and oxide aperture are mostly used in GaAs-based VCSELs while mesa-etch is the most common current confinement scheme applied in InP-based VCSELs.

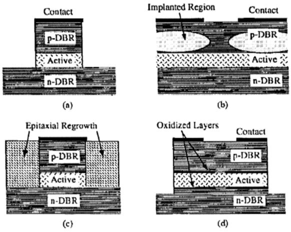

Figure 3.7: Schematics of some common VCSELs current confinement schemes (a) Mesa-etch (b) Proton implantation (c) Buried heterostructure and (d) Oxide aperture.

Various design approaches are being pursued in the development of long-wavelength VCSELs. The highest performance 1.55 μm VCSELs to date have been demonstrated by using strain compensated InGaAsP multi-QW (MQW) active region and wafer-fused GaAs/AlGaAs DBR mirrors [63]. A schematic of the device structure is shown in Figure 3.8. It consists of two MBE grown GaAs/AlGaAs mirrors which are double-fused to MOCVD grown InGaAsP active region.

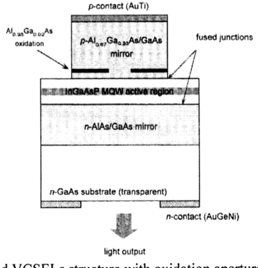

Figure 3.8: Double-fused VCSELs structure with oxidation aperture of AlGaAs.

3.7 VCSELs Applications

The total annual market for laser diode is huge and dominates the worldwide laser sale as exhibit in a graph chart attached in Appendix B. These applications are almost exclusively filled by EELs but VCSELs have potential usage for any of these applications. In order to displace EELs, VCSELs must produce equal or superior performance at a lower cost. The technology, production and manufacturing cost of EELs are well developed, thus displacing it will not be easy. However, the unique geometry of VCSELs promises lower processing and packaging cost. In addition, the special features of VCSELs are likely to open up entirely new applications such as laser arrays in communications, which is not addressed by EELs. VCSELs have been commercialized in short-distance data communications such as Gigabit Ethernet. Long-distance optical-fiber communications, however, make the attractive application target for VCSELs, where it represents the largest market for laser diode. The increasing emphasis on Wavelength-Division Multiplexing (WDM) and Fiber-to-the-House (FTTH) technologies suggests the potential use of VCSELs arrays with different wavelengths. Such arrays have been demonstrated at shorter wavelengths on GaAs-based VCSELs [79, 80]. Major efforts in the VCSELs development have been pursued by Honeywell, IBM, Hewlett Packard, Motorola, NTT and Siemens.